Fermi National Accelerator Laboratory

FERMILAB-Conf-94/014-E

CDF

Direct Photon Plus Charm Quark Production at CDF

Stephen Kuhlmann

Argonne National Laboratory
Argonne, Illinois 60439

Fermi National Accelerator Laboratory
P.O. Box 500, Batavia, Illinois 60510

January 1994

Published Proceedings *9th Topical Workshop on Proton-Antiproton Collider Physics*,
University of Tsukuba, Tsukuba, Japan, October 18-22, 1993

Disclaimer

CDF/PUB/JET/PUBLIC/2425
FERMILAB-CONF-94/014-E

Direct Photon Plus Charm Quark Production at CDF

Stephen Kuhlmann
Argonne National Laboratory
Argonne, Il. USA 60439

New measurements of direct photon production in association with a charm quark are presented. Comparisons are made with a QCD prediction.

1. Introduction

CDF has recently acquired large data samples of QCD jet and direct photon events. These are a significant improvement over the samples acquired in previous data runs, not only in terms of raw numbers of events, but in specialized triggers and new detector components that greatly enhance the physics capabilities.

From this new data sample 8 QCD jet and direct photon analyses were presented at the 1993 Lepton-Photon conference, and these were briefly reviewed in this talk as well. But there is neither space nor need to describe these analyses in this proceedings, as the Lepton-Photon proceedings themselves provide the best reference. In addition, there were two analyses presented at this conference that have never been shown before, both involving direct photon plus charm production. It is much more useful to use this space to detail these analyses in great detail, and that is what this paper will present.

2. Direct Photon+Charm Overview

In the direct photon compton process, a charm quark from the proton can interact with a gluon and give an outgoing photon plus charm quark. Thus this is a direct probe of the charm content of the proton. Very little is known about the flavor dependence of the sea quarks in nucleons, much less that of the heavier charm and bottom quarks. The main source of charm quarks inside the proton is expected to arise from gluon splitting described by perturbative QCD, this is what is included in standard sets of parton distributions. The main uncertainties in this arise from the amount of charm at the charm quark threshold, the so-called intrinsic component or non-perturbative component. How this component changes with scale would not necessarily follow perturbative QCD evolution either. Another motivation is that this component is becoming a larger component of the quark momenta in the proton as we go to higher energies, at the Tevatron it is roughly 10% of the total quark momenta, at the SSC it is 25%.

The first step in detecting direct photon plus charm events is to remove the π^0 backgrounds from the photons. This is done in the same way as the published CDF inclusive photon cross section, using the shower profile in our central shower maximum chambers [1]. Detecting the charm quark can be done in various ways. Full reconstruction of charmed mesons such as the D^0 and D^* is the most direct and convincing evidence for charm, but suffer from small branching ratios. The semi-leptonic decays of the charm quark give the

Published Proceedings 9th Topical Workshop on Proton-Antiproton Collider Physics, University of Tsukuba, Tsukuba-shi, Japan, October 18-22, 1993

best branching ratios but are less direct due to a longer decay chain and photon+lepton events could come from other sources, including new physics sources. Other methods include detecting the finite charm quark lifetime using the CDF secondary vertex detector. All of these are being pursued, the present results include full reconstruction of D^* mesons, as well as the muon semi-leptonic decays.

3. Direct Photon Sample

The direct photon trigger asked for isolated photons with p_T greater than 16 GeV. This trigger was unprescaled and collected more than 18 pb^{-1} of data, of which 15 pb^{-1} is being reported on in this paper. This is a high rate trigger, collecting more than 1 million photon candidates. The cuts applied to remove the majority of π^0 candidates are the same as detailed in [1]. The subsequent statistical subtraction of the remaining π^0 component is also the same as [1]. This is the sample from which evidence for the charm quark is searched for.

4. D* Detection Technique

In order to identify an event containing charm, we reconstruct D^{*+} in the channel of the sequential decay, $D^{*+} \rightarrow D^0\pi^+ \rightarrow K^-\pi^+\pi^+$(and its charged conjugate), and constrain the mass difference $\delta M = M(K^-\pi^+\pi^+) - M(K^-\pi^+)$. This method can eliminate the combinatorial background because of the small Q-value of the decay, $D^{*+} \rightarrow D^0\pi^+$. Charged tracks are looped over 3 times, with the mass assignments of both K and π applied. To reduce background, the following criteria are applied to the combinations:

Cuts		Loose Cut	Tight Cut
P_T of K from $D^0 \rightarrow K^-\pi^+$	$>$	0.4 GeV/c	1.0 GeV/c
P_T of π from $D^0 \rightarrow K^-\pi^+$	$>$	0.4 GeV/c	0.7 GeV/c
P_T of π from $D^{*+} \rightarrow D^0\pi^+$	$>$	0.4 GeV/c	0.4 GeV/c
$\lvert\cos\theta_H\rvert$	$<$	0.85	0.85

Loose and Tight Cuts		
1.64	$< \lvert\phi_{photon} - \phi_{track}\rvert <$	4.64
0.3	$< z = E_T^{K\pi\pi}/E_T^{photon} <$	1.3

where M_{D^0} is 1864.5 MeV/c^2 (P.D.G.) value, θ_H is the angle which is an angle between D^0 and K direction in D^0 rest frame.

The PYTHIA(V5.4) Monte Carlo plus a full detector simulation was used in order to determine these cut parameters. The charm+photon events were generated with the following input parameters: 1) Morfin-Tung Set 3 parton distribution with $Q^2 = M_T^{charm}/2$, 2) E_T of photon > 16 GeV, 3) $|\eta|$ of photon < 1.0, and 4) $|\eta|$ of charm < 4.0. Fig.1 shows the P_T distributions of the K and π are shown, along with arrows indicating the "tight" cuts. Note that these cuts are still quite efficient. The $K\pi$ mass distribution after detector simulation is shown in Fig.2, along with the arrows indicating the tight cuts.

5. Photon+D* Data Analysis

We now apply this D^* detection technique to the direct photon sample described above. The D^0 mass peak in this sample is shown in fig.3 with the set of loose cuts described earlier, and with $D^* - D^0$ mass difference constrained as shown in the figure. The D^0 peak is evident in the photon+π^0 and photon samples, but there is no peak in the π^0 sample. Fig.4 shows the same peaks with the tight cuts. The sideband regions are displayed in fig.5, no significant signals are seen here. Since we see a signal at the correct D^0 mass, and only in the photon sample (not in the sideband or π^0 samples), nor does the signal depend on the loose or tight cuts, we believe we are seeing photon+charm production. With this we can calculate the number of signal events observed above background and the photon+charm cross section.

Fig.6 shows a closer view of the $K\pi$ mass with the tight cuts and in the photon sample. The background is fitted as a function of $a + b \times (M_{K\pi} - c)$ except for the D^0 signal region of $1.835 < M_{K\pi} < 1.895\ GeV/c^2$. The photon+$D^{*\pm}$ candidates are subtracted using the fitted result. The number of $D^{*\pm}$ candidates is estimated to be:

$$N_{D^{*\pm}} = 15.78 \pm 7.46.$$

To derive the photon+charm cross section we need the efficiency for detecting the photon and the D^*. The total photon efficiency is 35%, as detailed in [1]. The D^* efficiency breaks down into three parts; 1) the fraction of kaons that do not decay in the tracking volume, 95.4%, 2) the acceptance for D^* to be produced centrally, along with the track P_T and mass cuts, 49.3%, and 3) the other cuts such as helicity, 84.8%. The total efficiency is 11.8% with a 20% systematic uncertainty.

The total cross-section of photon+charm production with the photon above 16 GeV is determined by the following formula:

$$\frac{(N_{D^{*+}} + N_{D^{*-}})/2}{\epsilon \times L \times P_{c \to D^{*+}} \times Br(D^{*+} \to D^0\pi^+ \to K^-\pi^+\pi^+)},$$

where $(N_{D^{*+}} + N_{D^{*-}})$ is the number of events observed in CDF data, L is the integrated luminosity, ϵ is the overall efficiency of this analysis, $P\ (c \to D^{*+})$ is the probability of forming D^{*+} from charm quark, and $Br(D^{*+} \to D^0\pi^+ \to K^-\pi^+\pi^+)$ is the branching ratio of the sequential decay of $D^{*+} \to D^0\pi^+ \to K^-\pi^+\pi^+$. The ALEPH collaboration measures the number of $P\ (c \to D^{*+}) \times Br\ (D^{*+} \to D^0\pi^+ \to K^-\pi^+\pi^+)$ to be 6.7 ± 0.4 (stat.) ± 0.7 (syst.) [2]. We use this number and uncertainty directly in this analysis. Each number in the above formula is summarized in the following table:

			stat. error	syst. error (%)
$N_{D^{*+}} + N_{D^{*-}}$	=	15.78	± 7.46	
ϵ	=	0.118	± 0.02	22
L	=	15.0		6.8
$P_{c \to D^{*+}} \times Br\ (D^{*+} \to D^0\pi^+ \to K^-\pi^+\pi^+)$	=	6.7×10^{-3}		12
			± 7.46	26 %

$$\sigma(\bar{p}p \to \gamma + charm + X; E_T^\gamma > 16\ GeV, |\eta^\gamma| < 0.9) = 665 \pm 314\ (stat.) \pm 173\ (syst.)\ pb.$$

The predicted cross-section from PYTHIA is 823 *pb*, within 1 standard deviation of the measurement. This PYTHIA prediction only uses the perturbative QCD prediction for the amount of charm in the proton, there is no additional non-perturbative piece added. There are additional processes that can give rise to photon+charm production, such as photon+gluon with the gluon splitting into a charm-anticharm pair, or the process where the photon is radiated off the charm quark. These need to be studied in more detail to understand their effect on the measured cross section.

6. Photon+Muon Production

As mentioned earlier, better statistics can be gained by measuring the semi-leptonic decays of the charm quark. We present here a recent study of the muon decay. The central muon detectors were upgraded before this last data run, with more than 3 interaction lengths of steel added and a redundant set of muon chambers behind this steel. In this analysis we require a track above 4 GeV P_T in the central tracking chamber, matched in $r - \phi$ to both the old central muon chambers and in addition to the new chambers. This matching we believe has removed the interactive pion punchthru backgrounds that were prevalent with the old system. Evidence for this removal is figure 7, which shows a very clean minimum ionizing distribution in the central hadron calorimeter.

There are two classes of backgrounds that remain. There is the non-interactive punchthru, and then the pion and kaon decays-in-flight. These are modeled by taking the measured charged particle spectrum in the photon events, figure 8, and convoluting this with the known decay features of the pion and kaon. The result of this is shown in figure 9, along with the total measured photon+muon spectrum. The breakdown of non-interactive punchthru and decays-in-flight is shown, and a clear excess of events above these predicted backgrounds is seen. This excess is the true photon+muon signal. This signal is shown again in figure 10, with the sum total of the backgrounds displayed. There is an excess of 75 events above the background, and this is consistent within statistics with the number of D^* events shown earlier, once relative branching ratios and acceptances are taken into account.

7. Conclusions and Future Prospects

Clear evidence for photon+charm production is shown using D^* and muon signals, and is in agreement with a PYTHIA QCD prediction. In the future other decay modes of the D^* will be added. Also, using the rest of the CDF muon acceptance, as well as lowering the P_T cutoff to 2.5 GeV, should lead to a measurement with 400 photon+muon events above background. This can be doubled if photon+electron events are added too. Thus a very high statistics (of order 800 events) measurement is possible with the data sample already on tape. With this, detailed studies of the different physical processes that give rise to photon+charm production can be studied.

References

[1] CDF Collab., F. Abe et al, Phys. Rev. D 48(1993) 2998.
CDF Collab., F. Abe et al, Phys. Rev. Letters 46(1992) 2734.

[2] ALEPH Collab., D. Decamp et al, Phys. Lett. B266(1991) 218.

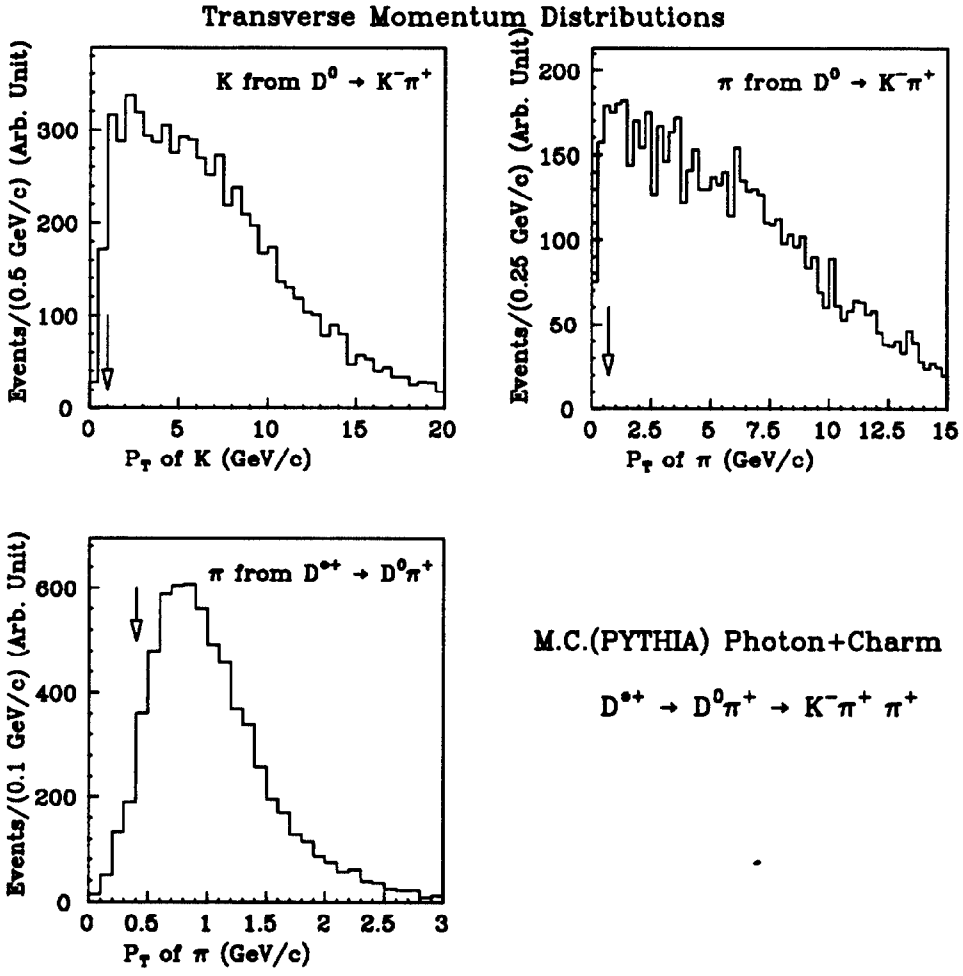

Figure 1: Simulated track transverse momentum distributions for K,$\pi(D^0 \rightarrow K\pi)$ and $\pi(D^{*+} \rightarrow D^0\pi^+)$. The arrows indicate the "tight" set of cuts described in the text.

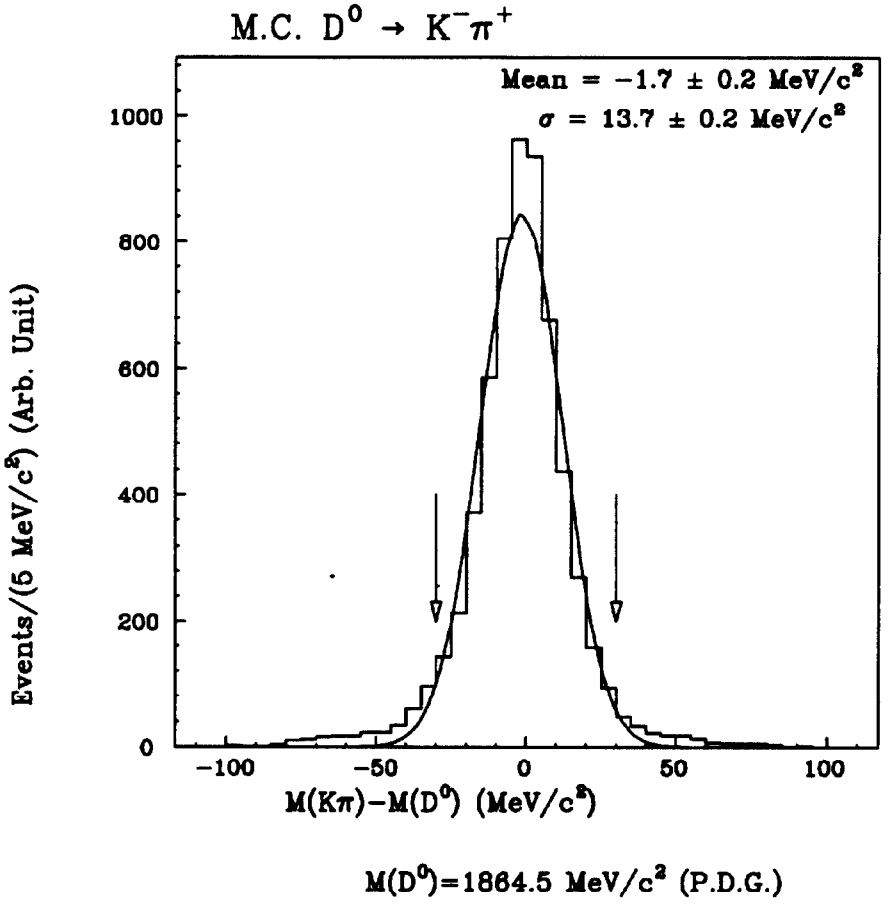

Figure 2: Simulated $\dot{D}^{\sigma} \rightarrow K^{-}\pi^{+}$ mass distribution, indicating the mass resolution and width of peak we expect to observe.

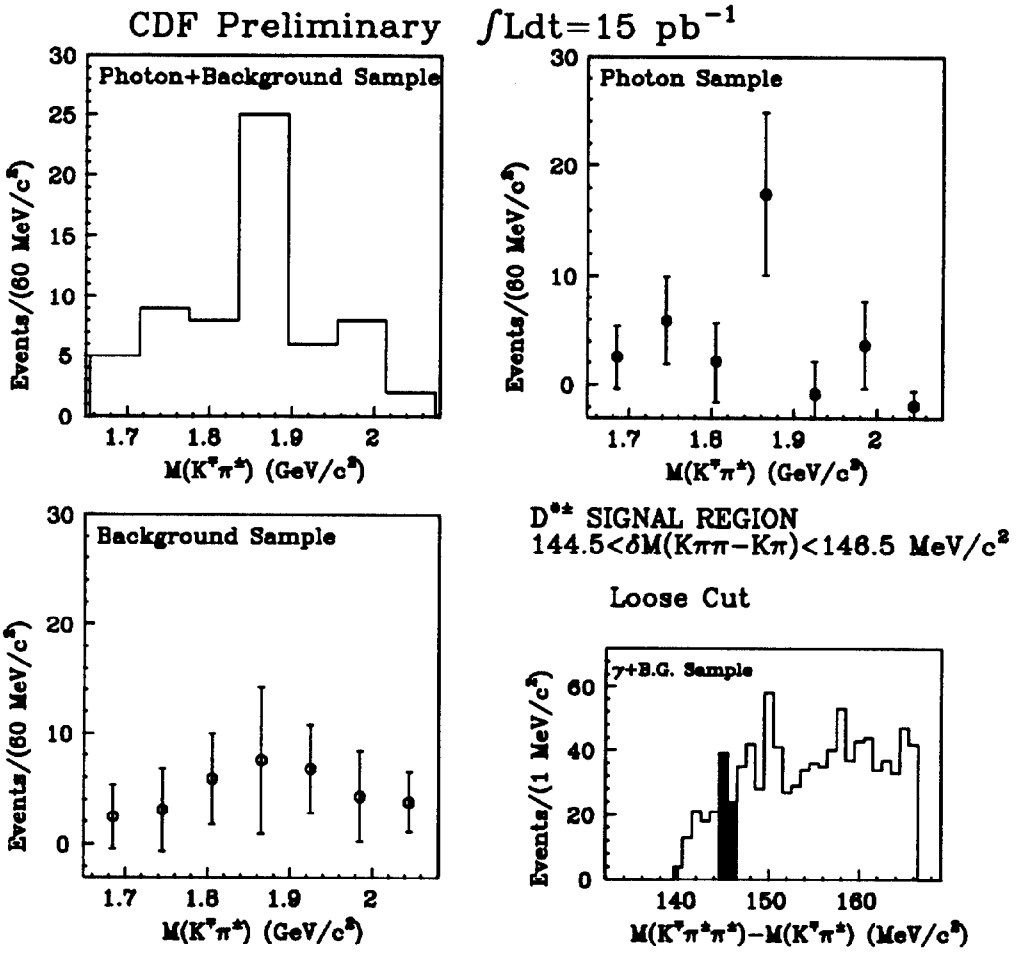

Figure 3: The $K\pi$ mass distributions with the "loose" set of cuts that are described in the text. The $D^* - D^0$ mass difference is constrained as shown in the lower right. The upper left is the photon+π^0 sample, the upper right the photons, the lower left the π^0.

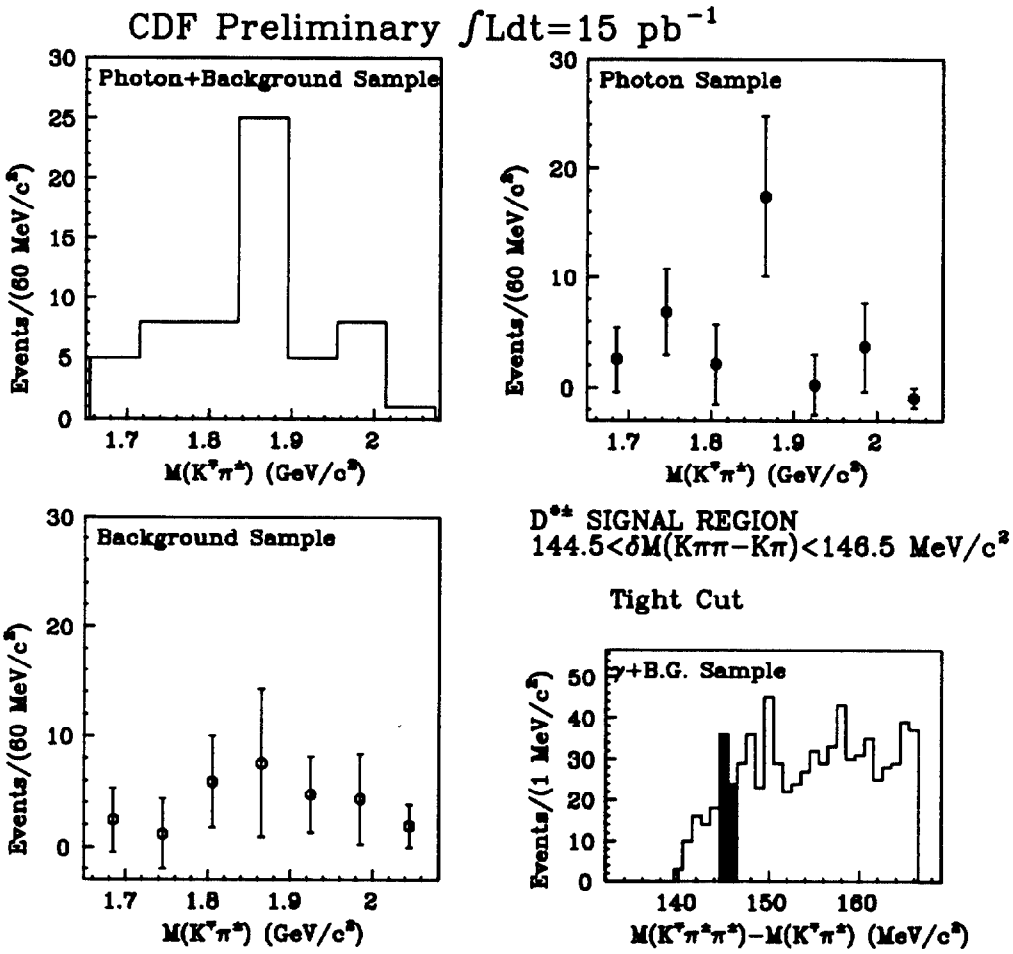

Figure 4: The $K\pi$ mass distributions as in the last figure but with the "tight" set of cuts described in the text.

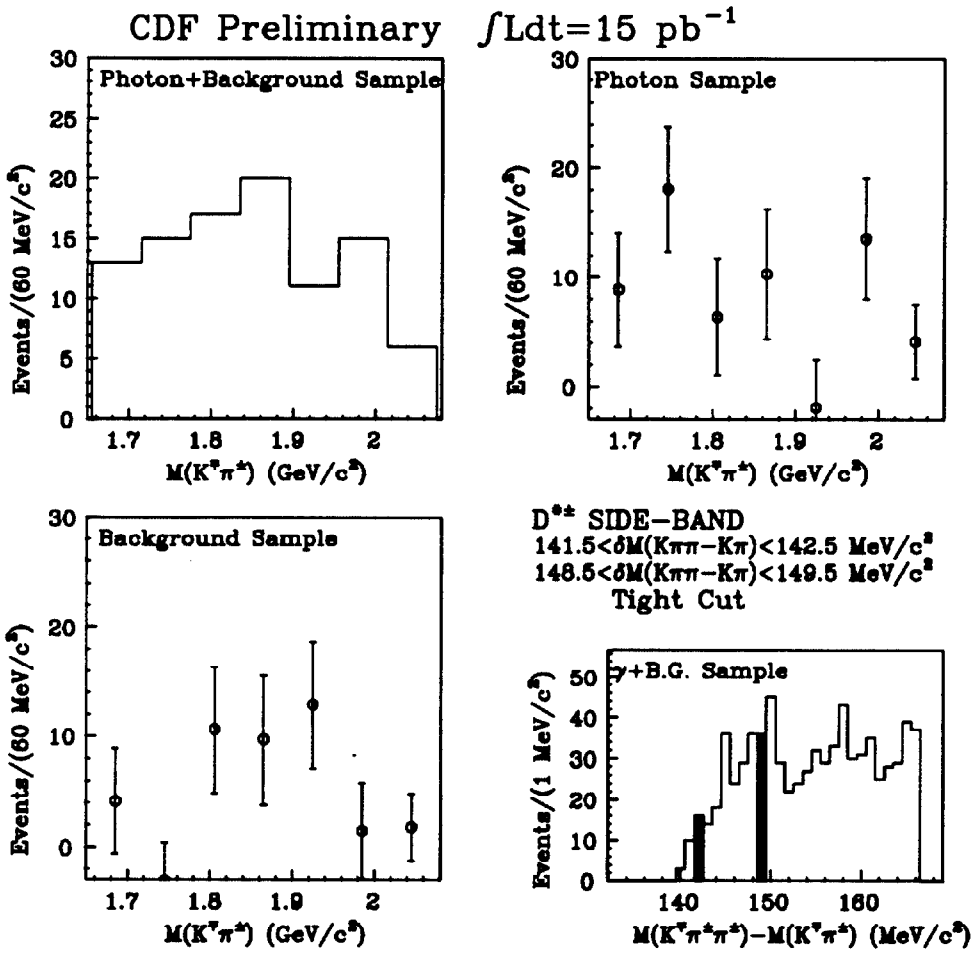

Figure 5: The $K\pi$ mass distributions with the tight cuts except this uses the side-band region of the D^* signal

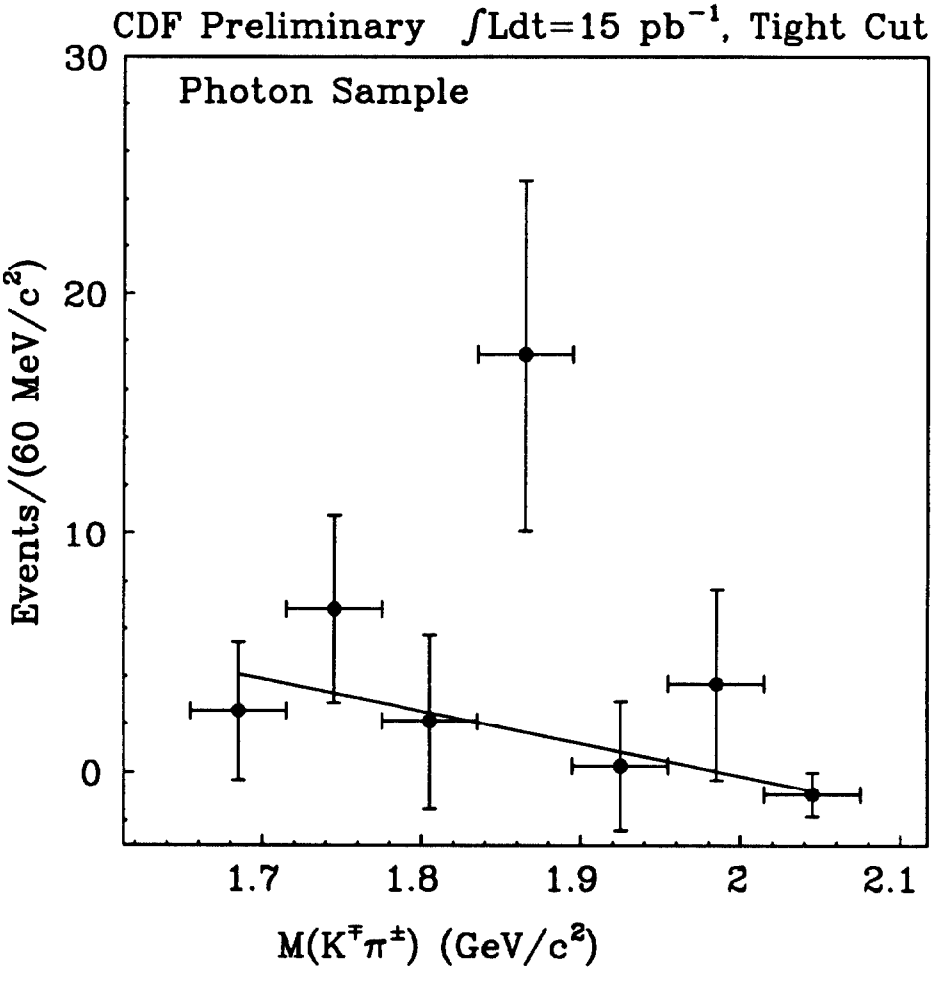

Figure 6: A blowup of the $K\pi$ mass distribution with the tight cuts. The line indicates the fitted background.

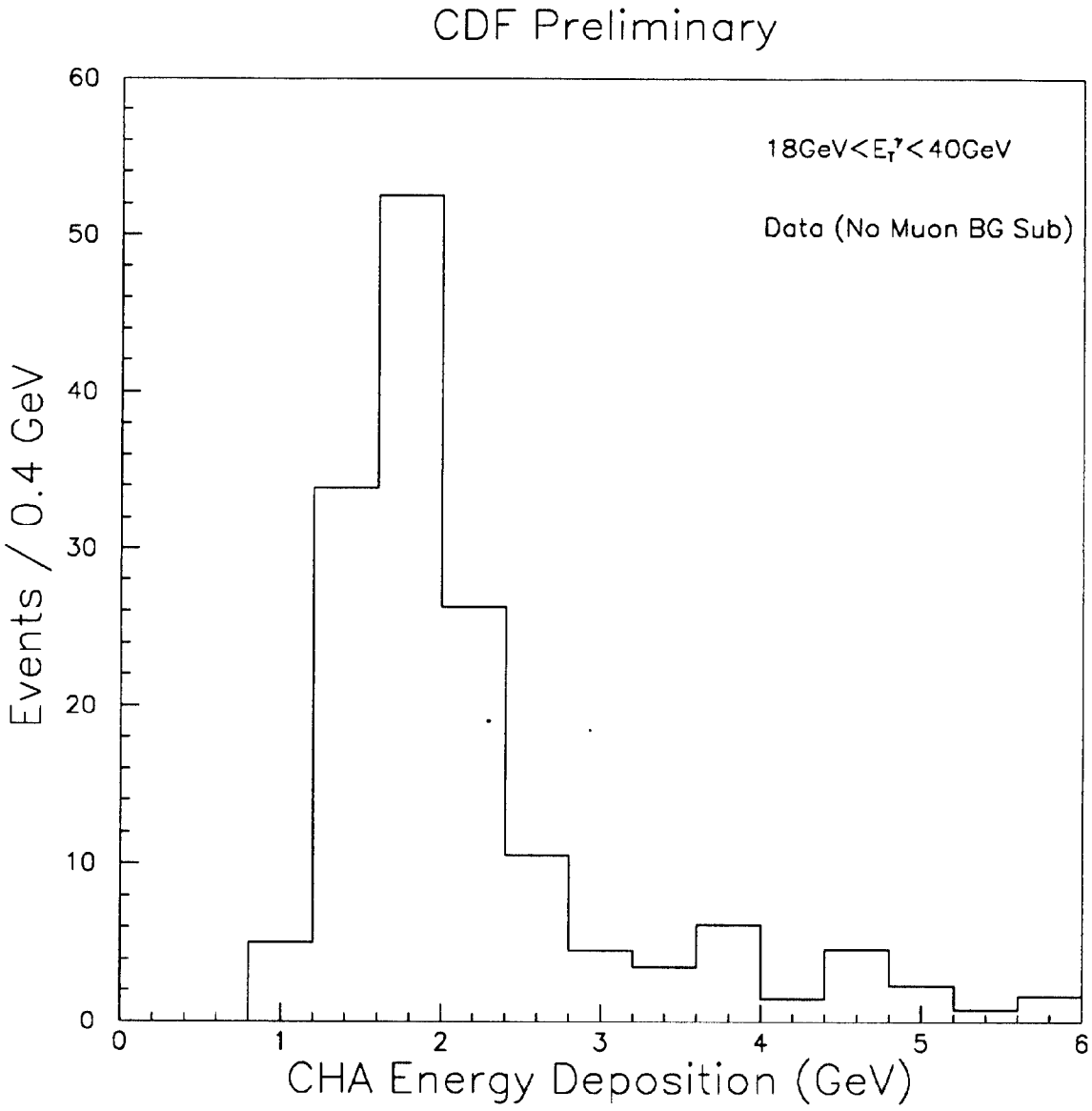

Figure 7: The central hadron calorimeter energy distribution for the photon+muon sample, indicating a minimum ionizing peak.

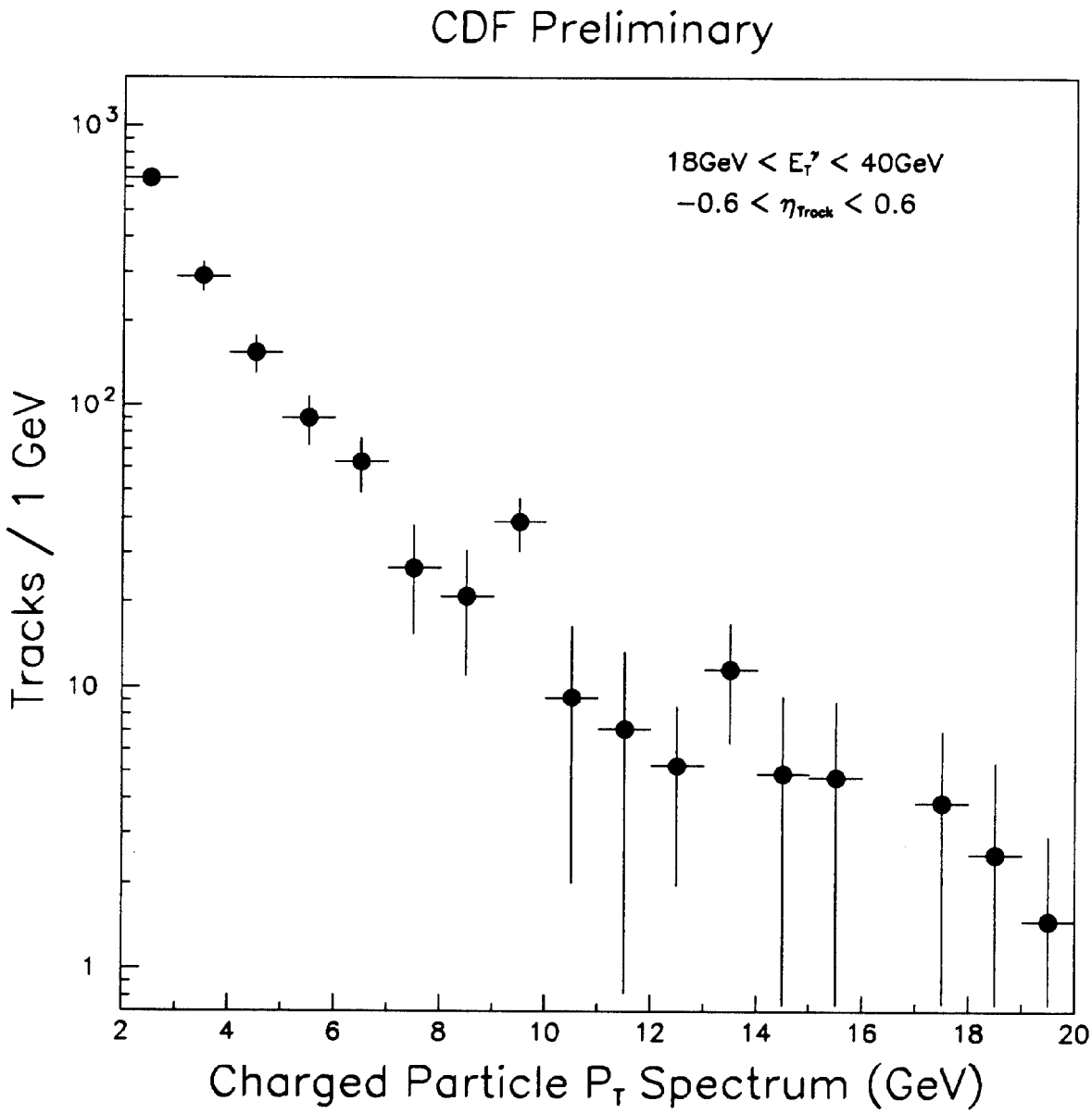

Figure 8: The charged particle P_T spectrum in the photon sample. From this is derived the decay-in-flight and non-interactive punchthru backgrounds.

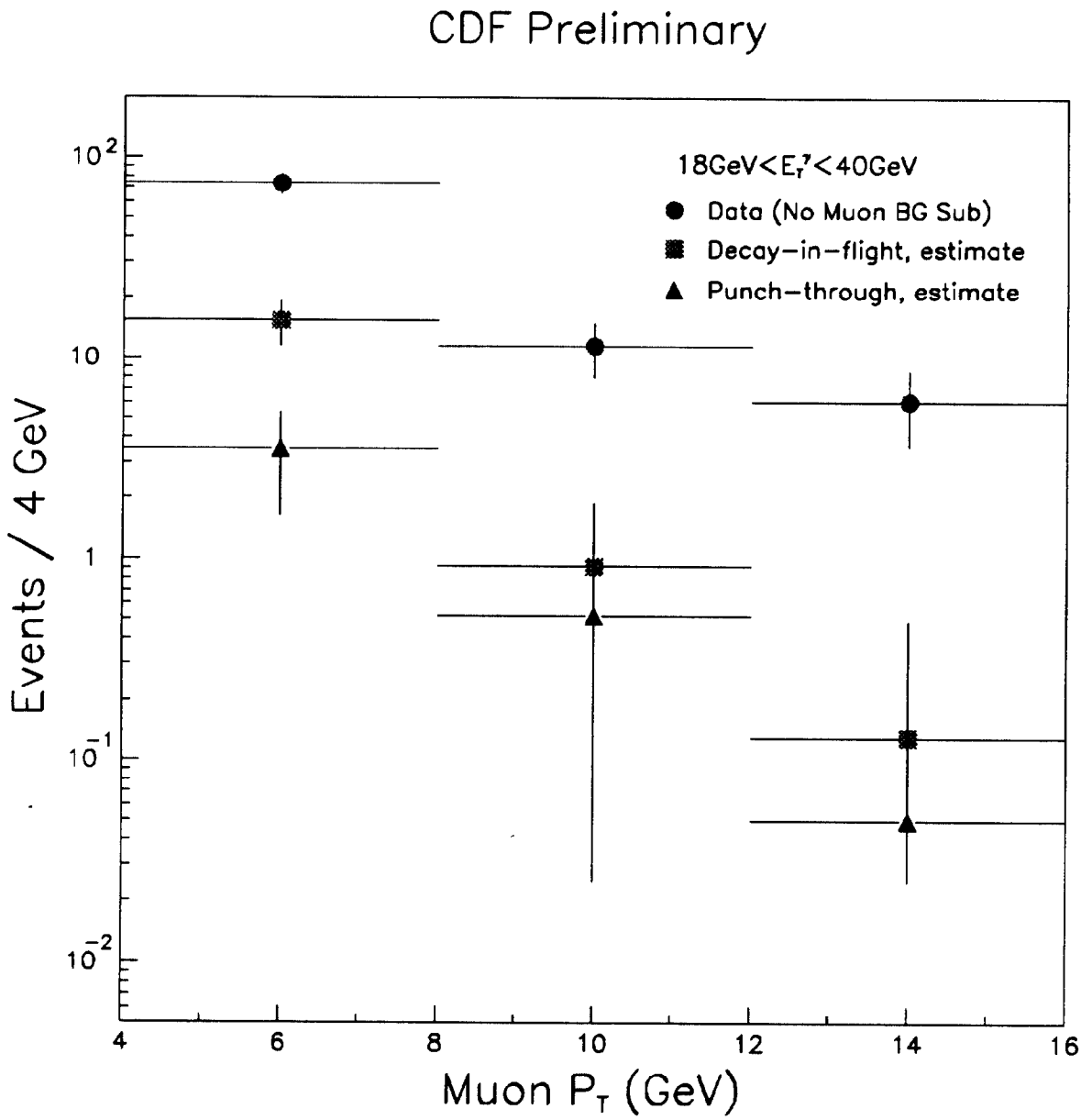

Figure 9: The muon P_T spectrum in photon events, along with the expected backgrounds from decays-in-flight and non-interactive punchthru.

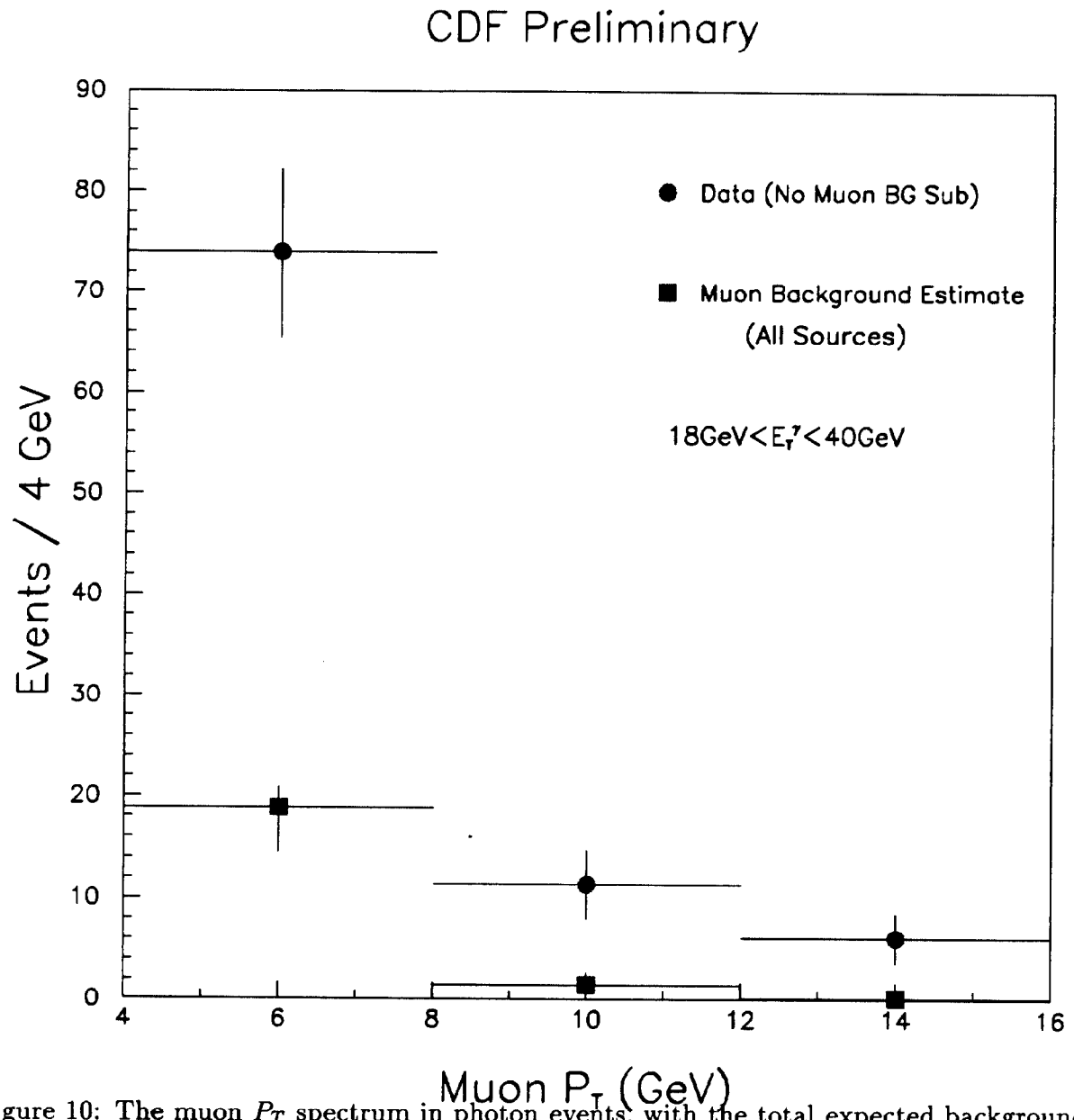

Figure 10: The muon P_T spectrum in photon events, with the total expected backgrounds. A clear excess over background is seen.